Multi-Ion Space Plasma Research: Two highlights

I. Plasma structures and boundaries in solar wind interaction with non-magnetized bodies

II. Origin of coherent large-amplitude waves in multi-ion space plasmas

K. Sauer*

Max-Planck-Institut für Aeronomie,
KatlenburgLindau, Germany

* in close cooperation with E. Dubinin (MPAe)
and partly with A. Lipatov and J. McKenzie

Multi-Ion Space Plasma Research:

I. Plasma structures and boundaries in solar wind interaction with non-magnetized bodies

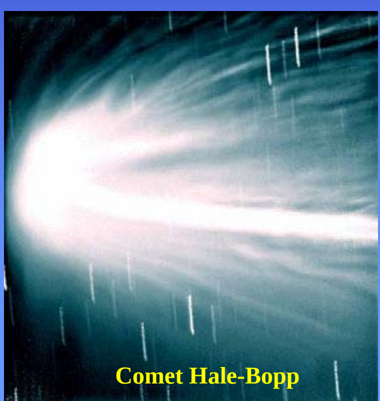

Comet Hale-Bopp

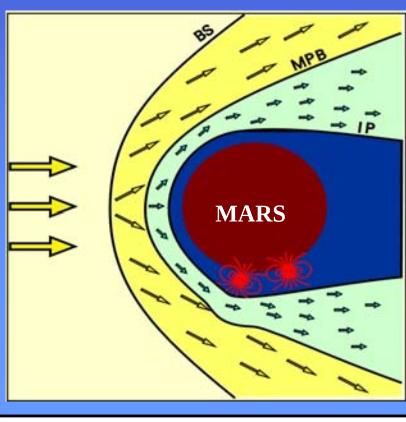

MISPR

Multi-Ion Space Plasma Research:

I. Plasma structures and boundaries in solar wind interaction with non-magnetized bodies

- **Introduction:**
  History of Mars Plasma Research
- **Two-fluid model of interaction**
- **Numerical results**
- **The MPB at Mars - a new type of plasma boundary**
- **Implications to ROSETTA, MARS-EXPRESS and CASSINI**

MISPR

Ion acoustic waves in an Ar-He plasma

Theory: Fried et al., 1971; **Experiment:** Tran and Coquerand, 1976

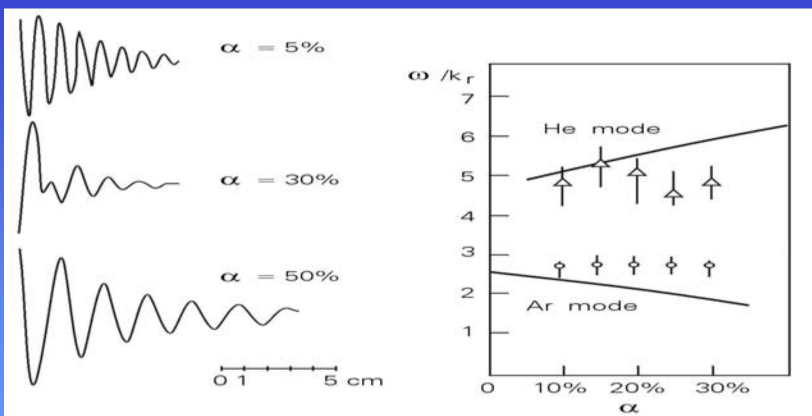

Left: experimental wave pattern for different concentration α. The interference pattern for α = 30% is due to the super-position of the two wave modes.

Right: phase velocity of the two ion-acoustic modes versus the concentration α

Dust-acoustic waves in a Q machine
(Barkan et al., 1996)

Dust-acoustic waves (Rao, Shukla and Yu ;1990):

$$v_{ph} = \sqrt{\left(\frac{k(T_e + T_i)}{m_d}\frac{n_d}{n_p}Z^2\right)}$$

Differential streaming between protons and α-particles in the solar wind

Helios: Marsch et al., 1982
Ulysses: Neugebauer et al., 1994, 1996
Wind: Steinberg et al., 1996

$V_{\alpha p} = |\mathbf{v}_p - \mathbf{v}_\alpha|$

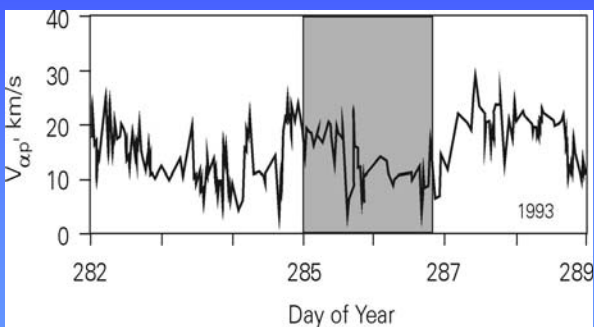

Temporal variation of $v_{\alpha p}$ for one week of Ulysses data (Neugebauer et al., 1996).

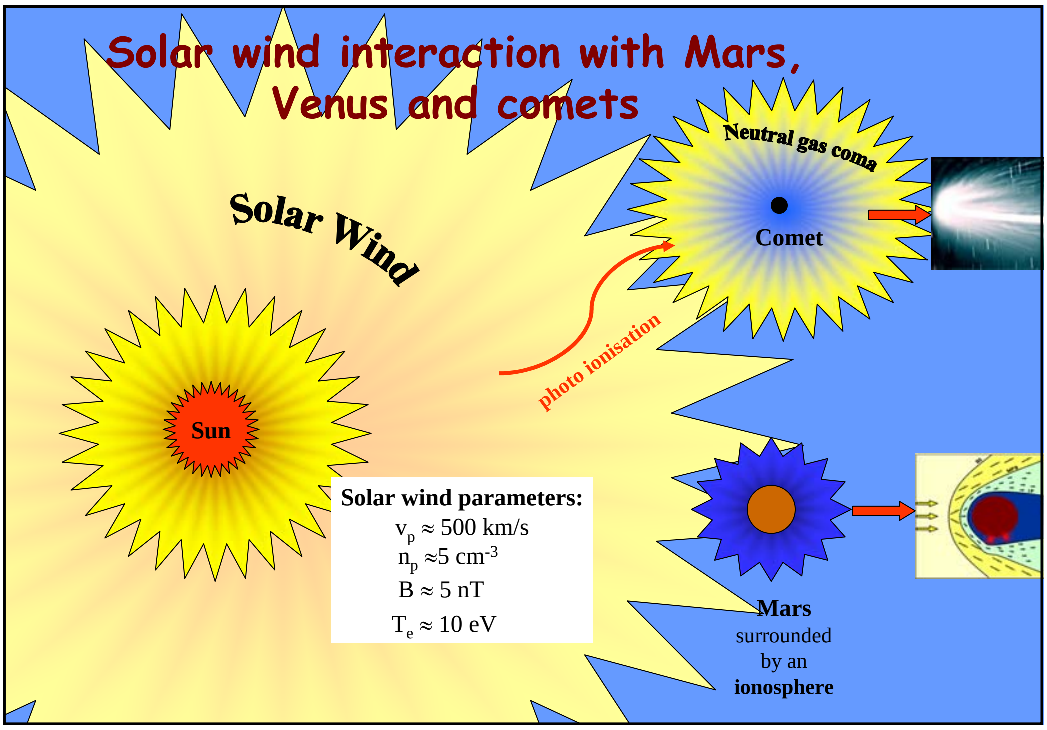
Solar wind interaction with Mars, Venus and comets
Solar Wind
Neutral gas coma
Comet
photo ionisation
Sun
Solar wind parameters:
$v_p \approx 500$ km/s
$n_p \approx 5$ cm^{-3}
$B \approx 5$ nT
$T_e \approx 10$ eV
Mars
surrounded
by an
ionosphere


MISPR
Dynamic solar wind and comet observation by Lasco on SOHO
C3 1996/04/30 01:35

The cometary plasma boundaries

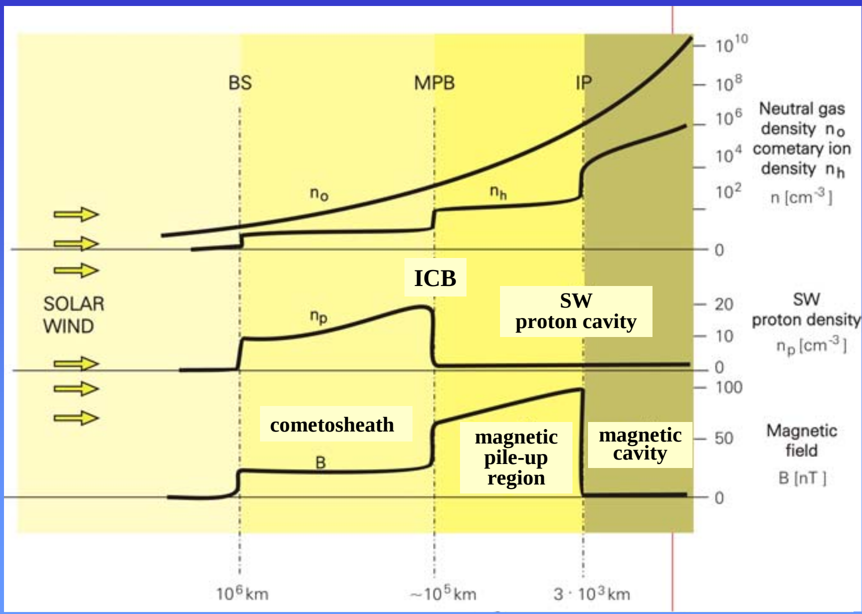

Plasma boundaries at comets and Mars

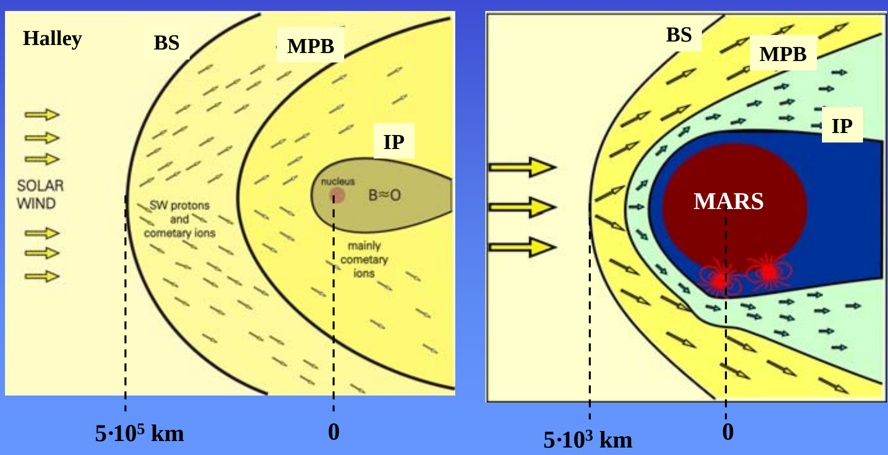

Scientific aspects of solar wind - Mars interaction

Study of **fundamental processes of plasma-plasma interaction** which are relevant for many other situations: comets, moons (Titan), asteroids, Pluto, dust rings, etc.

Mars dehydration:
loss of water by solar wind - atmosphere coupling;
1-10 m of surface water in 4.5 billion years.

Space weather: generation of high energetic particles, especially by CMEs (no shielding by an intrinsic magnetic field).

Solar wind scavenging of the martian atmosphere => dehydration

Mars Express: ASPERA-3 will do global imaging and *in-situ* measurements of:

Inflow — solar wind

Outflow — planetary wind

using

Energetic neutral atom cameras and plasma (ion+electron) spectrometers

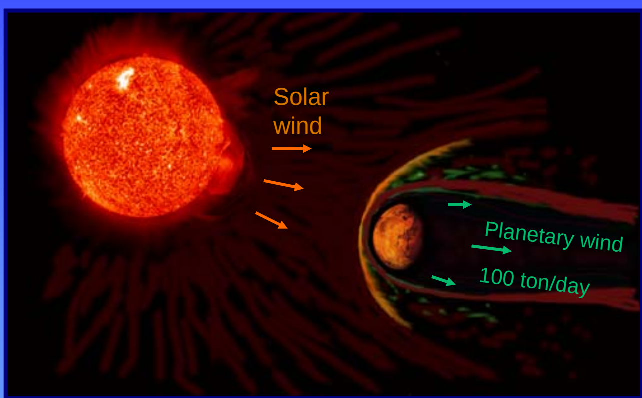

Scientific aspects of solar wind - Mars interaction

Study of **fundamental processes of plasma-plasma interaction** which are relevant for many other situations: comets, moons (Titan), asteroids, Pluto, dust, etc.

Mars dehydration:
loss of water by solar wind - atmosphere coupling;
1-10 m of surface water in 4.5 billion years.

Space weather: flux of high energetic particles, especially by CMEs (no shielding by an intrinsic magnetic field).

History of Mars Plasma Research

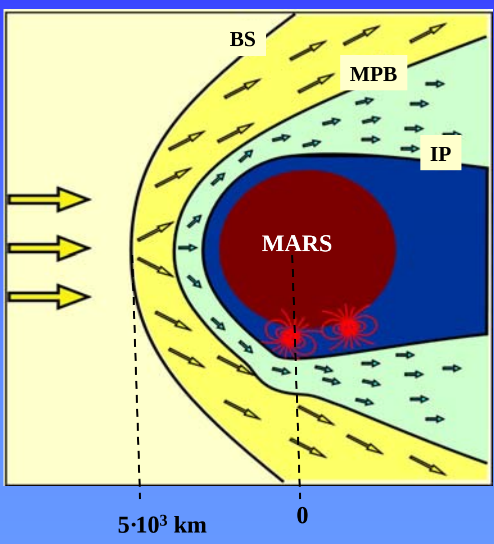

Our present view

MISPR

Mars-2 observations in 1972

(Dolginov and Gringauz, 1972)

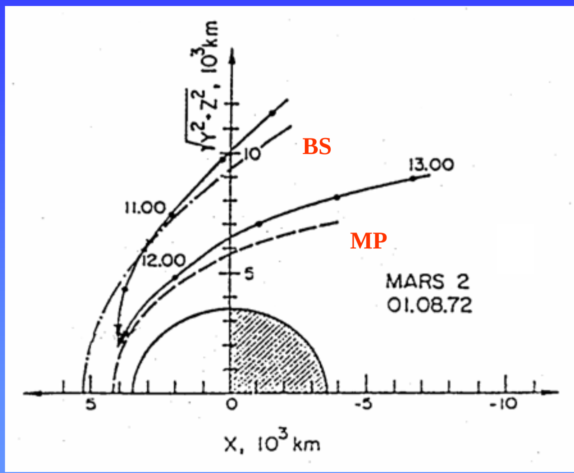

The spacecraft crossed the bow shock (BS) and the obstacle boundary (magnetopause = MP)

MISPR

Mars-2 observations in 1972

(Dolginov and Gringauz, 1972)

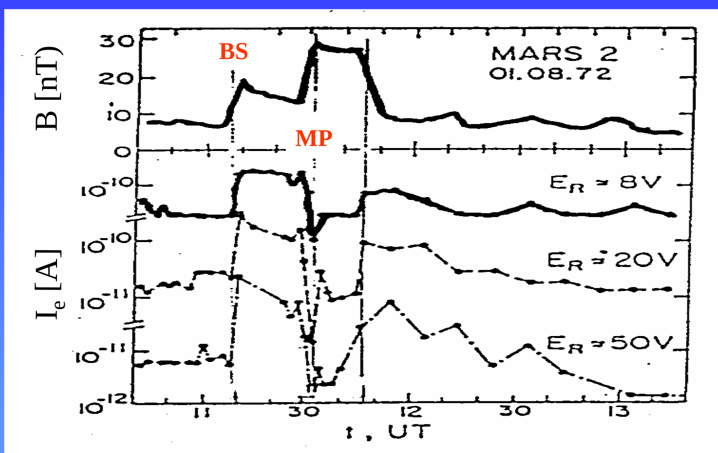

Variation of the magnetic field B and the electron current I_e at crossing the bow shock (BS) and the obstacle boundary (magnetopause = MP)

Obstacle boundary in classical MHD models

MISPR

The solar wind dynamic pressure is balanced by

ionospheric thermal pressure:

$\rho v^2 = n_e k T_e$

(Ionopause)

For $T_e \approx 1$ eV, a density of $n_e \geq 10^4$ cm^{-3} is required. The ionosphere of Mars is not dense enough to reach such a density at about 500 km where the obstacle boundary is observed. Therefore, the observed boundary is not an Ionopause.

intrinsic magnetic pressure:

$\rho v^2 = B^2/2\mu_0$

(Magnetopause)

From the observed location of the obstacle boundary in a subsolar height of about 500 km a magnetic moment of Mars of about

$M \geq 10^{12}$ T·m^3

was estimated.

History of the Mars magnetic moment 1965 - 2000

MISPR

From position and shape of the obstacle boundary (MP) a magnetic moment of $M \geq 10^{12}$ T·m^3 was estimated.

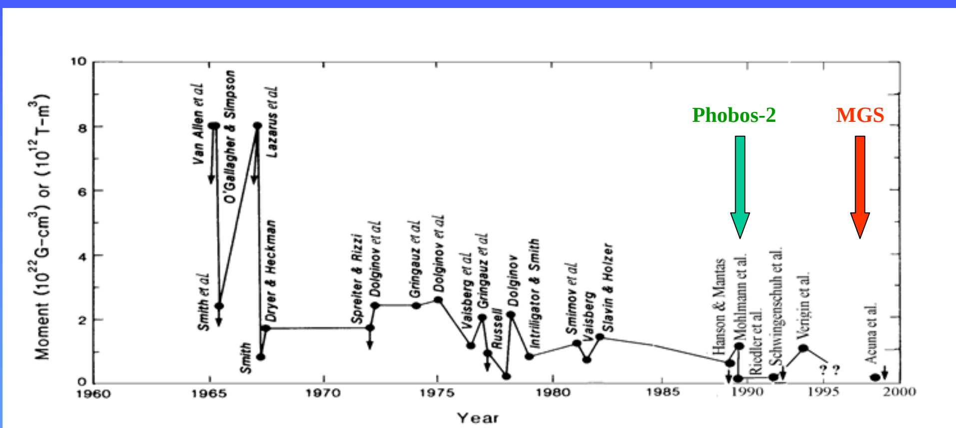

The Phobos-2 mission in 1989

The spacecraft approached Mars down to about 850 km during 4 elliptical orbits, nearly one month in a circular orbit, approached the Phobos moon up to 200 km.

It was equipped with important instruments for plasma research: magnetometer (MAGMA, FGMM), electron and ion spectrometers (ASPERA, TAUS), sounders for low- and high- frequency plasma waves

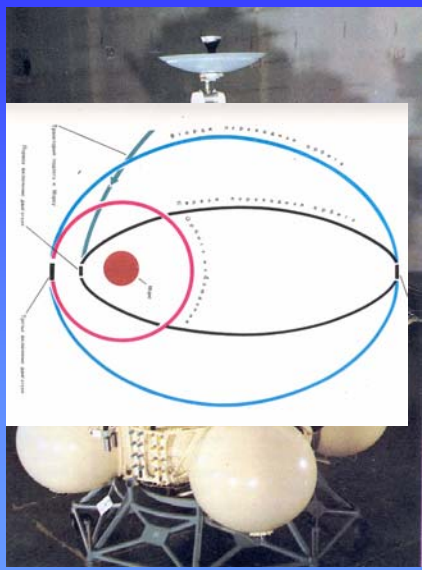

Observation of the Ion Composition Boundary (ICB) by Phobos-2

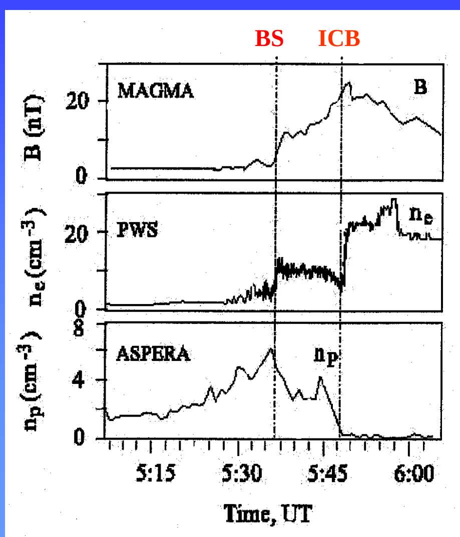

Signatures of the ICB:

- SW proton density decreases
- electron density n_e sharply increases which -because of charge neutrality - means an abrupt increase of the planetary ion density: Protons are replaced by heavy ions.

MISPR

Observation of the MPB/ICB in large distances by Phobos-2 (1989)

(≥20 000 km)

Jump of the magnetic field:
MPB
Change of ion composition:

- SW protons outside
- planetary ions (oxygen) inside

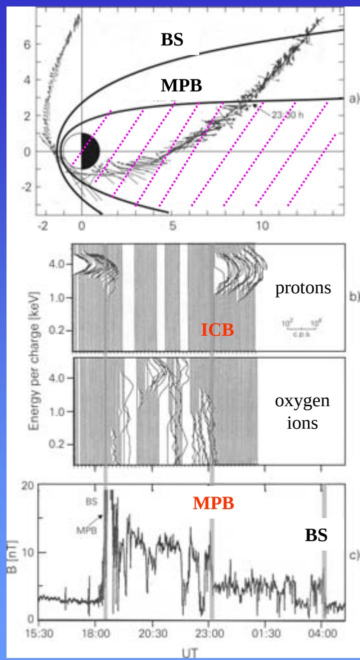

MPAE

MISPR

Observation of the MPB/ICB in large distances by Phobos-2

(≥20 000 km)

Jump of the magnetic field:
MPB
Change of ion composition:

- SW protons outside
- planetary ions (oxygen) inside

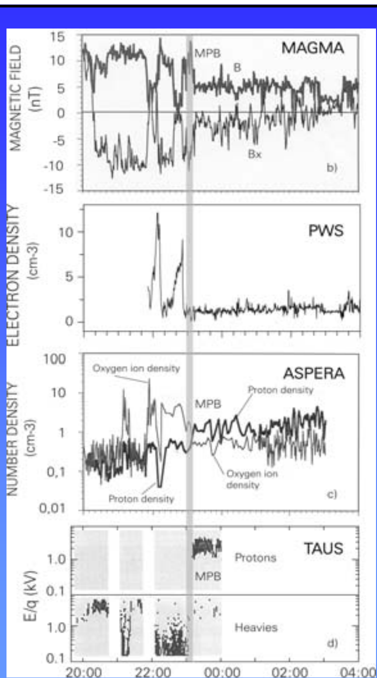

MPAE

Phobos-2 observations of the Ion Composition Boundary

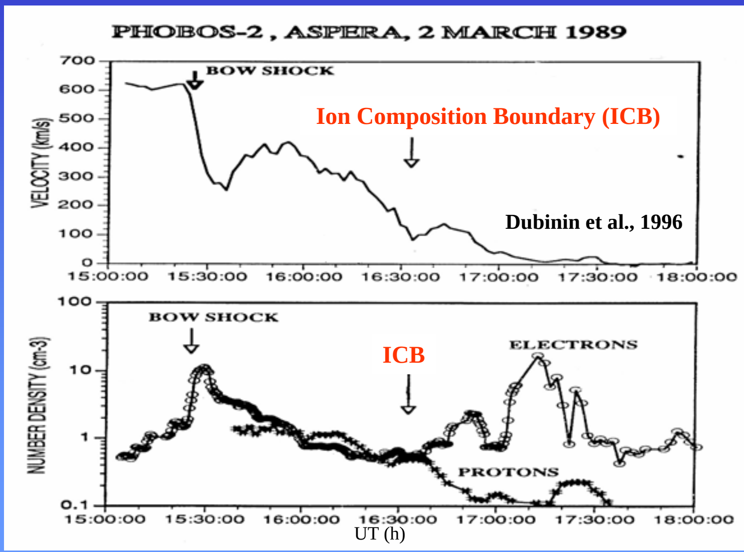

Mars Global Surveyor -

its contribution to Mars plasma research

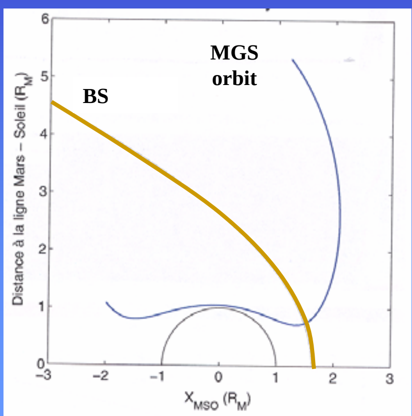

Most important:

MGS went down to Mars up to about **150 km**. The spacecraft carries a **magnetometer** and an **electron spectrometer**. It crossed the **ionopause** and from the measured magnetic field a moment of **$M \approx 10^{11}$ T·m^3** was determined. This value is more than one order of magnitude weaker than estimated before.

The Magnetic Pile-up Boundary at Mars and comet Halley

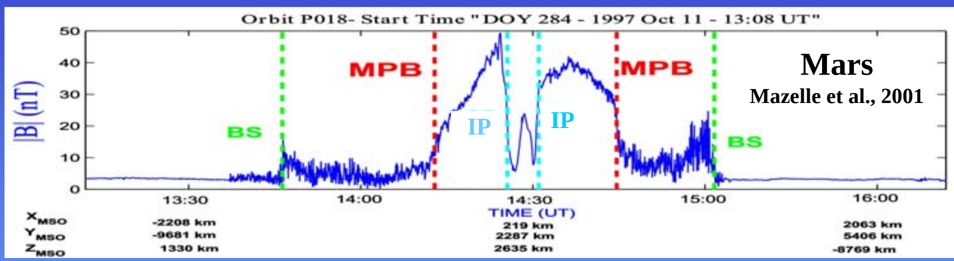

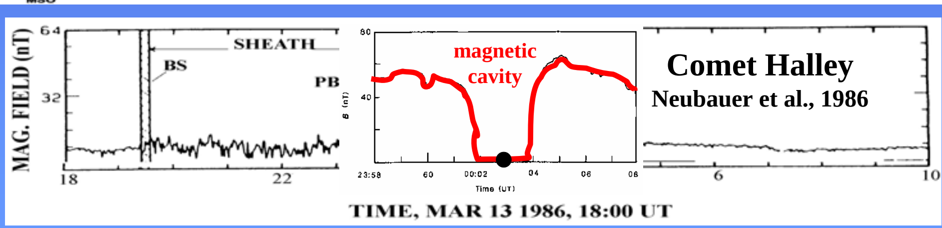

First attempts to find the ICB in two-ion fluid simulations

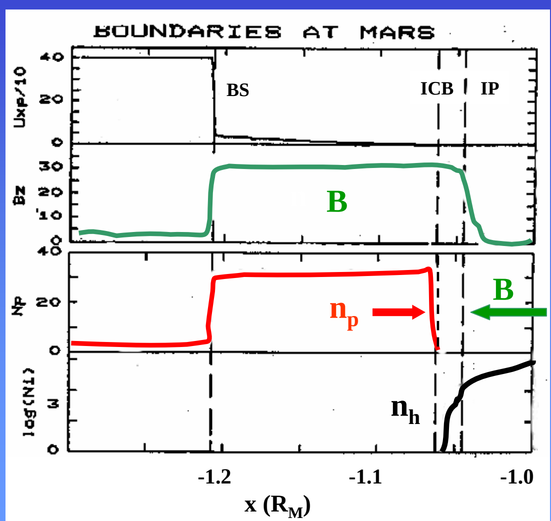

1D two-ion fluid simulations with lateral effects

First attempts to find the ICB in two-ion fluid simulations

1990

Plasma boundaries at Mars discovered by the Phobos 2 magnetometers

K. SAUER (1), TH. ROATSCH (1), U. MOTSCHMANN (1), D. MÖHLMANN (1), K. SCHWINGENSCHUH (2), and W. RIEDLER (2)

(1) Institut für Kosmosforschung, Akademie der Wissenschaften der DDR, Rudower Chaussee 5, Berlin, DDR-1199
(2) Institut für Weltraumforschung, Österreichische Akademie der Wissenschaften, Inffeldgasse 12, Graz, A-8010, Austria

ABSTRACT. ......This boundary is interpreted as a multi-ion contact discontinuity where the protons are deflected by the Lorentz force arising from the relative motion between both ion fluids. The magnetic field penetrates the ICB.......

Annales Geophysicae, 1990, **8**, (10), 661-670.

Indication of three plasma boundaries from the Phobos-2 observations; 1D bi-ion fluid simulations with lateral effects

Further steps in two-ion fluid simulations

1994

First theoretical evidence of an Ion Composition Boundary (ICB) in 2D simulations of solar wind massloading.

(The protonopause - an ion composition boundary in the magnetosheath of comets, Venus and Mars; Sauer et al., *GRL*)

1999 (after MGS)

Improved 2D two-ion fluid model (inclusion of thermal effects) showing the Magnetic Pile-up Boundary (MPB) at the same location as the ICB.

(The nature of the Martian obstacle boundary; Sauer and Dubinin, *Adv. Space Res.*)

2001-2003

Joint Phobos - MGS ISSI workshops: Mars book (Kluwer) + *Space Science Review* will be published in spring of 2004.

Theoretical methods for describing multi-ion plasmas

Linear theory:
Dispersion of LF multi-ion waves (fluid and kinetic models)

Numerical simulations:

(1) 1D and 2D bi-ion fluid simulations

(2) 1D and 2D bi-ion hybrid code simulations

Stationary nonlinear waves:
Oscillitons - a new type of solitary structure, origin of coherent waves

The two-ion fluid Hall-MHD model

Protons (p) and ***heavy ions*** (h) are considered as separate fluids which are coupled by electromagnetic forces

Electrons are mass less

Charge neutrality: $n_e = n_p + n_h$

No collisions

The system of basic equations consists of

- 2 continuity equations
- 2 momentum equations
- Faraday's law
- Energy equation for electrons

Solar wind flow though an heavy-ion cloud, simple model of electrostatic interaction

Situation at t=0:

solar wind

no magnetic field

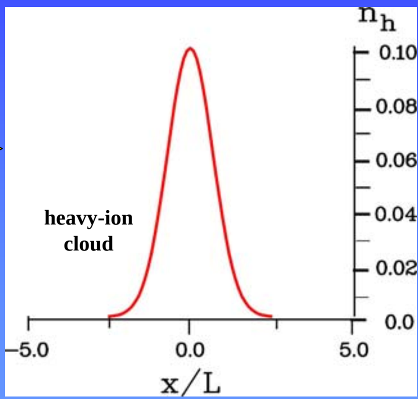

cold ions, warm electrons:

$$\frac{\partial}{\partial t} n_p + \frac{\partial}{\partial x}(n_p v_{px}) = 0$$

$$\frac{\partial}{\partial t}(n_p v_{px}) + \frac{\partial}{\partial x}(n_p v_{px}^2) = \frac{e\, n_p}{m_p} E_x$$

$$\frac{\partial}{\partial t} n_h + \frac{\partial}{\partial x}(n_h v_{hx}) = 0$$

$$\frac{\partial}{\partial t}(n_h v_{hx}) + \frac{\partial}{\partial x}(n_h v_{hx}^2) = \frac{e\, n_h}{m_h} E_x$$

$$E = -\frac{1}{e\, n_e}\frac{\partial}{\partial x} p_e \qquad m_e = 0$$

$$\frac{\partial}{\partial t} p_e + \frac{\partial}{\partial x}(v_{ex} p_e) + (\gamma - 1) p_e \frac{\partial}{\partial x} v_{ex} = 0 .$$

$$n_e = n_p + n_h \qquad v_{ex} = (n_p v_{px} + n_h v_{hx})/n_e$$

Solar wind flow though an heavy-ion cloud, simple model of electrostatic interaction

The interaction strongly depends on the **Mach number** of the incoming plasma flow

Solar wind flow though an heavy-ion cloud: simple model of electrostatic interaction

Supersonic flow:
M_s = 2.0

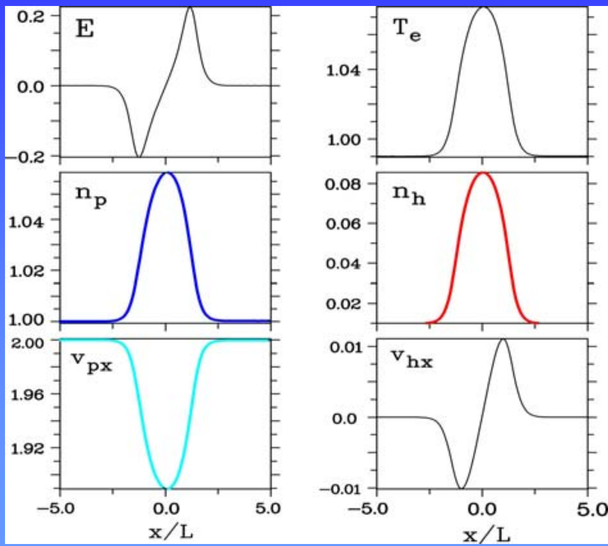

Solar wind flow though an heavy-ion cloud: simple model of electrostatic interaction

Subsonic flow:
M_s = 0.5

The flow is accelerated within the cloud: Laval nozzle effect

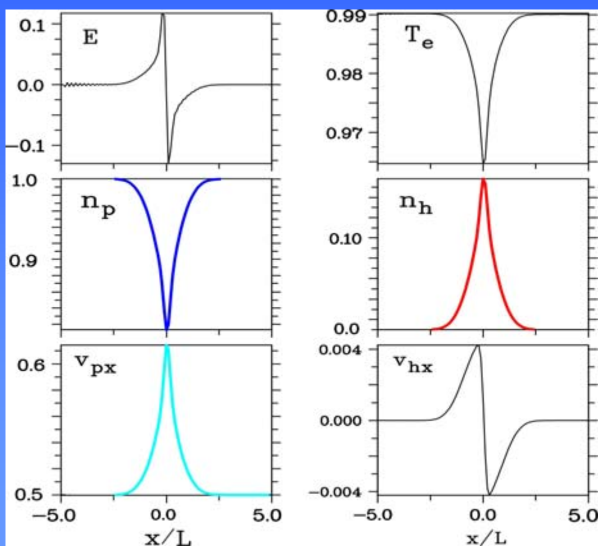

Solar wind flow though an heavy-ion cloud: hybrid code simulations

Sub-Alfvenic flow: $M_A = 0.1$

The flow is accelerated within the cloud

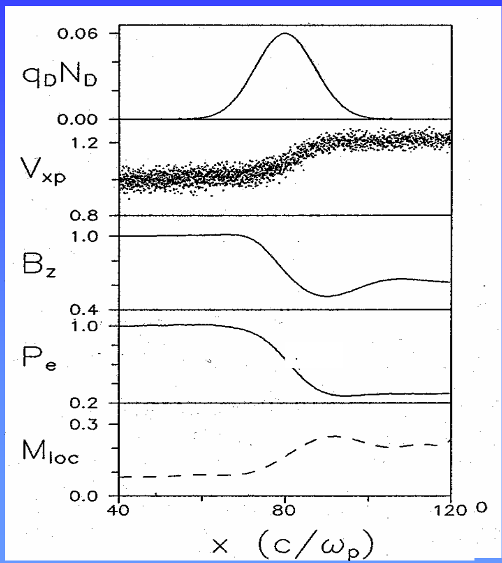

Motschmann, Sauer and Roatsch, 1992

Fluid description in the mass-less electron approximation

$$\frac{\partial}{\partial t}(n_p \mathbf{v}_p) + \nabla \cdot (n_p \mathbf{v}_p \mathbf{v}_p + \frac{P_p}{m_p}) = \frac{e\, n_p}{m_p}\left(\mathbf{E} + \mathbf{v}_p \mathbf{x} \mathbf{B}\right)$$

$$\mathbf{E} = - \frac{1}{e\, n_e} \nabla p_e - \mathbf{v}_e \mathbf{x} \mathbf{B}$$

approximation of mass-less electrons: $m_e=0$

Ampere's law is used to eliminate v_e

$$\nabla \mathbf{x} \mathbf{B} = - \mu_0 \, \mathbf{j}$$

$$\mathbf{j} = - e\, n_e v_e + n_p v_p + n_h v_h$$

Electron-proton plasma

$$\mathbf{v}_e = \mathbf{v}_p - \frac{1}{\mu_0 \, e \, n_e} \nabla \mathbf{x} \mathbf{B}$$

charge neutrality: $n_e = n_p$

Two-ion plasma

$$\mathbf{v}_e = \frac{n_p \mathbf{v}_p + n_n \mathbf{v}_h}{n_e} - \frac{1}{\mu_0 \, e \, n_e} \nabla \mathbf{x} \mathbf{B}$$

charge neutrality: $n_e = n_p + n_h$

Equation of motion in single- and two-ion fluid description

Single-ion (proton) plasma

$$\frac{\partial}{\partial t}(n_p m_p \mathbf{v}_p) + \nabla \cdot (n_p m_p \mathbf{v}_p \mathbf{v}_p + P_p) = \left[-\nabla \left(\left(P_e + \frac{B^2}{2\mu_0}\right)\mathbf{I} - \frac{\mathbf{BB}}{\mu_0} \right) \right]$$

Two-ion plasma

$$\frac{\partial}{\partial t}(n_p m_p \mathbf{v}_p) + \nabla \cdot (n_p m_p \mathbf{v}_p \mathbf{v}_p + P_p) =$$

$$\frac{n_p}{n_e}\left[e\, n_h (\mathbf{v}_p - \mathbf{v}_h)\mathrm{x}\mathbf{B} - \nabla \left(\left(P_e + \frac{B^2}{2\mu_0}\right)\mathbf{I} - \frac{\mathbf{BB}}{\mu_0} \right) \right]$$

gyro-radius effects

charge neutrality: $n_e = n_p + n_h$

Magnetic field equation

Faraday's law:

$$\frac{\partial \mathbf{B}}{\partial t} + \nabla \,\mathrm{x}\, \mathbf{E} = 0$$

$$\mathbf{E} = -\frac{1}{e\, n_e} \nabla p_e - \mathbf{v}_e \mathrm{x} \mathbf{B}$$

single-ion plasma

$$\mathbf{v}_e = \mathbf{v}_p - \frac{1}{\mu_0\, e\, n_e} \nabla \mathrm{x} \mathbf{B}$$

$$\frac{\partial \mathbf{B}}{\partial t} + \nabla \mathrm{x} \left[\mathbf{v}_p \mathrm{x} \mathbf{B} - \frac{\mathbf{B} \cdot \nabla \mathbf{B}}{e\, n_e\, \mu_0} \right] = 0$$

Hall term

two-ion plasma

$$\mathbf{v}_e = \frac{n_p \mathbf{v}_p + n_h \mathbf{v}_h}{n_e} - \frac{1}{\mu_0\, e\, n_e} \nabla\, \mathrm{x}\mathbf{B}$$

$$\frac{\partial \mathbf{B}}{\partial t} + \nabla \mathrm{x} \left[\frac{1}{n_e} (n_p \mathbf{v}_p + n_h \mathbf{v}_h)\, \mathrm{x}\mathbf{B} - \frac{\mathbf{B} \cdot \nabla \mathbf{B}}{e\, n_e\, \mu_0} \right] = 0$$

charge neutrality: $n_e = n_p + n_h$

Hall term

The two-ion Hall-MHD equations

Continuity and momentum equations of protons and heavies
(p→ h, h → p)

$$\frac{\partial}{\partial t} n_p + \nabla \cdot (n_p \mathbf{v}_p) = 0$$

$$\frac{\partial}{\partial t}(n_p \mathbf{v}_p) + \nabla \cdot (n_p \mathbf{v}_p \mathbf{v}_p + P_p / m_p) =$$
$$\frac{1}{m_p}\frac{n_p}{n_e}\left[e\, n_h (\mathbf{v}_p - \mathbf{v}_h) \mathbf{x} \mathbf{B} - \nabla\left((P_e + \frac{B^2}{2\mu_0})\mathbf{I} - \frac{\mathbf{BB}}{\mu_0} \right)\right]$$

Faraday's law

$$\frac{\partial \mathbf{B}}{\partial t} + \nabla \mathbf{x} \left[\frac{1}{n_e}\left(n_p \mathbf{v}_p + n_h \mathbf{v}_h\right) \mathbf{x} \mathbf{B} - \frac{\mathbf{B} \cdot \nabla \mathbf{B}}{e\, n_e\, \mu_0} \right] = 0$$

Electron energy equation

$$\frac{\partial}{\partial t} P_e + \nabla \cdot (\mathbf{v}_e P_e) + (\gamma - 1) P_e \, \nabla \cdot \mathbf{v}_e = 0 \, .$$

with

$$n_e = n_p + n_h \, , \qquad \mathbf{v}_e = \frac{n_p \mathbf{v}_p + n_h \mathbf{v}_h}{n_e} - \frac{\nabla \mathbf{x} \mathbf{B}}{n_e \mu_0}$$

2D hybrid simulation of solar wind - comet interaction

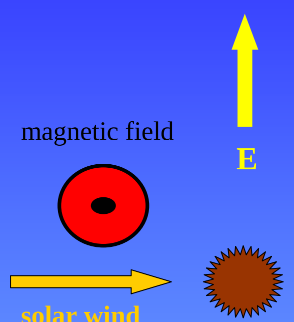

heavy ion source: weakly outgassing comet (Wirtanen at 3 AU)

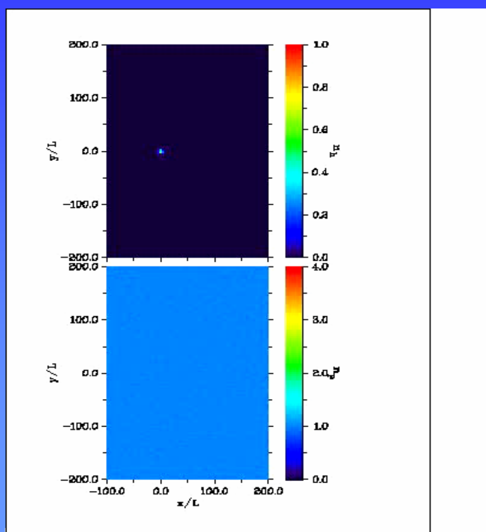

Lipatov and Sauer, 1997

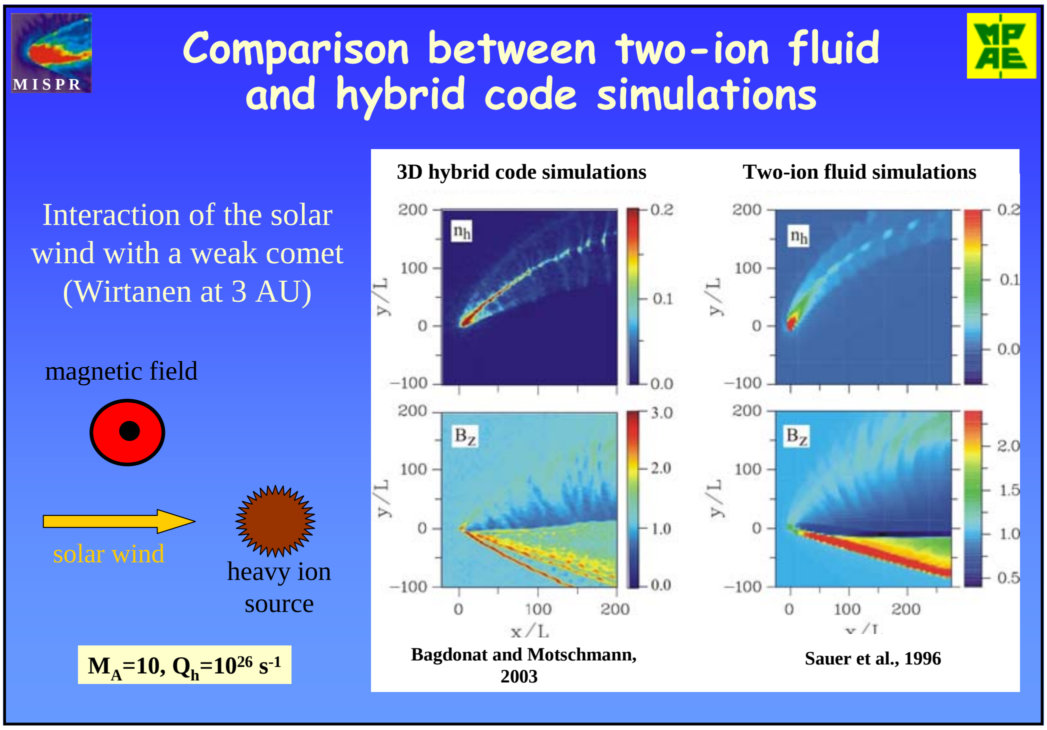
MISPR
Comparison between two-ion fluid and hybrid code simulations
Interaction of the solar wind with a weak comet (Wirtanen at 3 AU)
magnetic field
solar wind
heavy ion source
$M_A=10$, $Q_h=10^{26}$ s^{-1}
3D hybrid code simulations
Two-ion fluid simulations
n_h
B_z
y/L
x/L
Bagdonat and Motschmann, 2003
Sauer et al., 1996

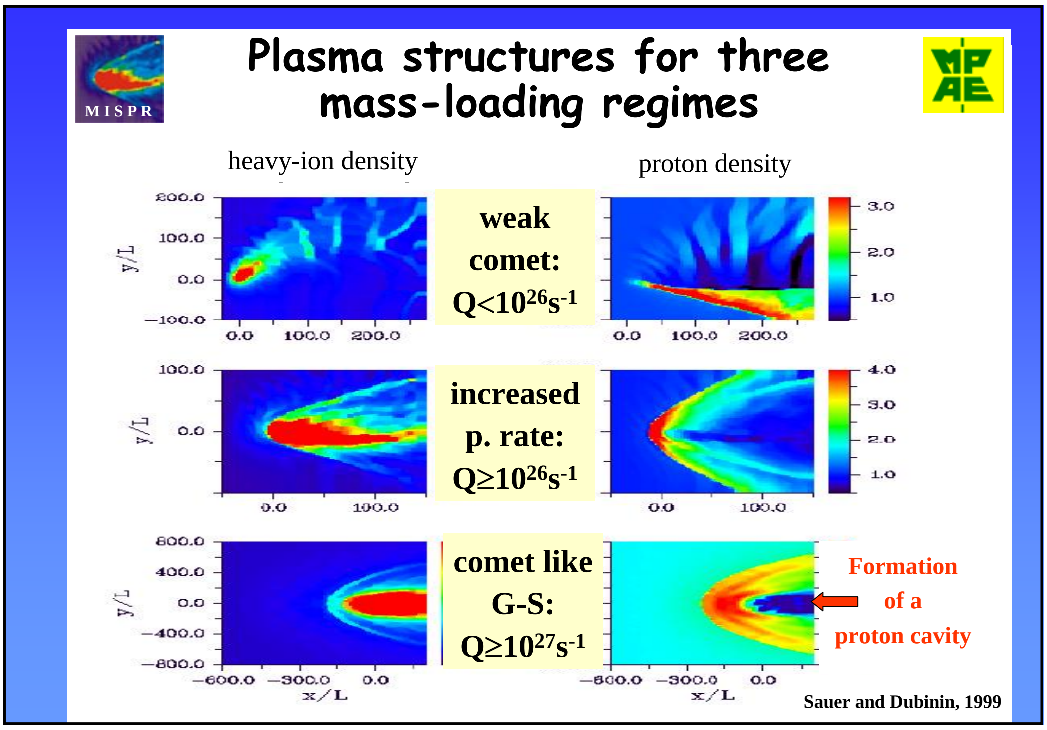
MISPR
Plasma structures for three mass-loading regimes
heavy-ion density
proton density
weak comet: $Q<10^{26}s^{-1}$
increased p. rate: $Q\geq10^{26}s^{-1}$
comet like G-S: $Q\geq10^{27}s^{-1}$
Formation of a proton cavity
y/L
x/L
Sauer and Dubinin, 1999

MISPR

Two-fluid modeling of solar wind interaction with the Martian exospheric plasma

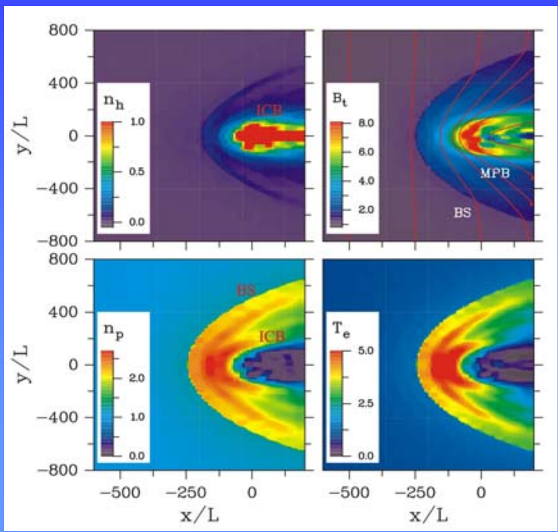

A proton cavity is formed. At the boundary separating solar wind protons from exospheric oxygen ions (ICB = Ion Composition Boundary) the magnetic field piles up (MPB)

Sauer and Dubinin, 1999

MISPR

Comparison between Phobos-2 observations and two-fluid modeling (elliptical orbit)

Phobos-2 observations   2-fluid modeling

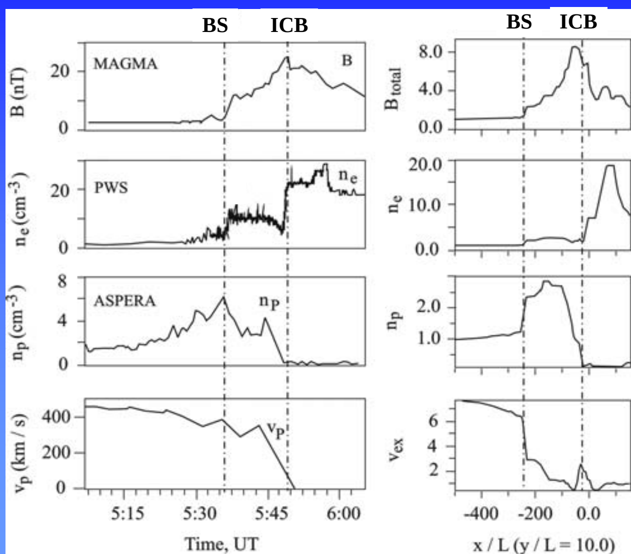

Comparison between Phobos-2 observations and two-fluid modeling (circular orbit)

Phobos-2 observations

2-fluid modeling

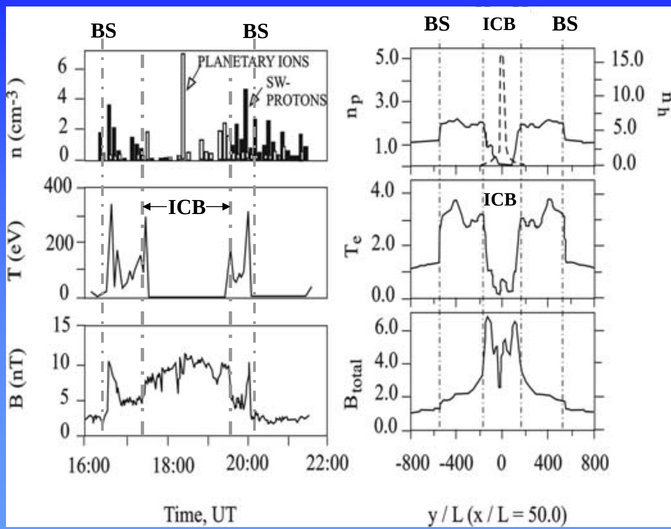

Hybrid simulations: Formation of a proton cavity

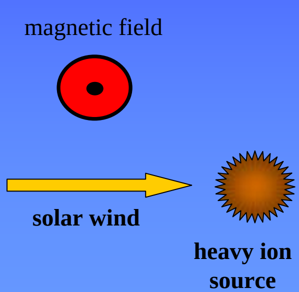

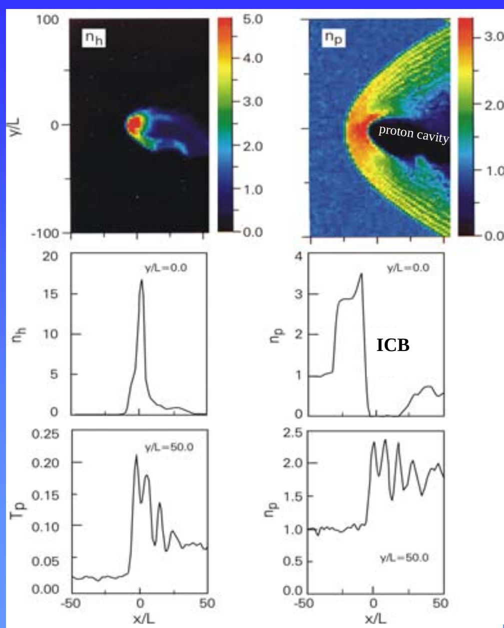

Lipatov and Sauer, 1997

3D hybrid simulations of SW interaction with unmagnetized planets

MISPR

Planetary ions are distributed over a sphere, no ionospheric profiles: Shimazu, 2001

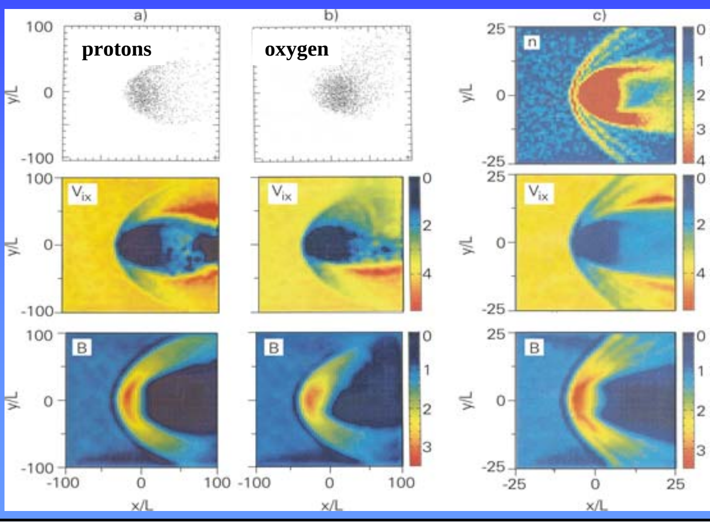

Important results:

(1) Formation of an ICB

(2) Multiple shock-structure

(3) Plasma acceleration at the flanks

3D hybrid simulations of solar wind - Mars interaction

MISPR

(Bößwetter, Bagdonat, Motschmann - TU Braunschweig
K. Sauer - MPAe; 2004)

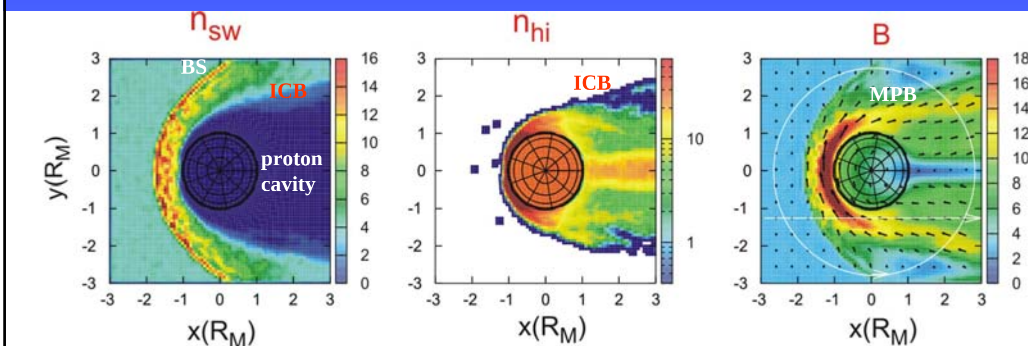

Main signatures of interaction are seen. Location of BS and MPB/ICB are in good agreement with the observations.

The Ion Composition Boundary (ICB) - a new type of plasma boundary

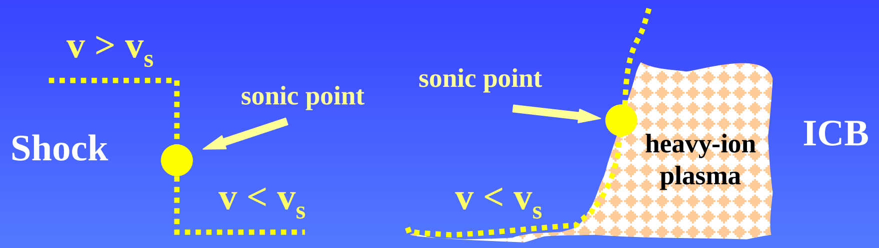

A **shock** is formed if the "**supersonic**" flow goes through the "sonic point": $v = v_s$

An **ICB** is formed if the "**subsonic**" two-ion flow becomes accelerated and goes through the "generalized sonic point": $v = v_s(n_p, n_h, v_h, \beta_e, ...)$

Formation of a proton cavity in a subsonic flow

heavy-ion cloud: $n_h \leq 1.5\, n_{p0}$

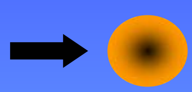

proton flow ($M_s = 0.4$)

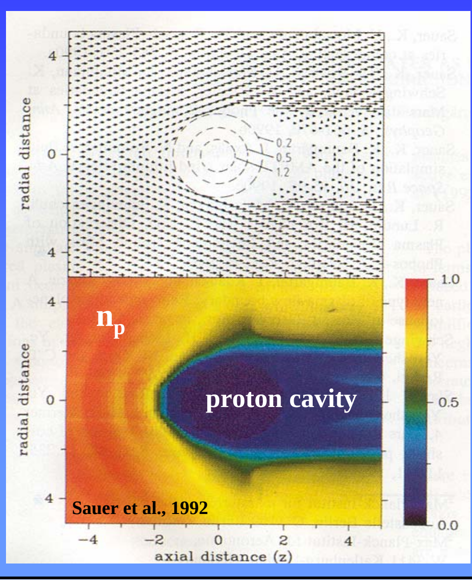

Plasma acceleration at the flanks of an impenetrable heavy-ion cloud

heavy-ion cloud

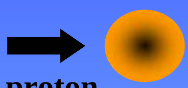

proton flow (M_s= 0.4)

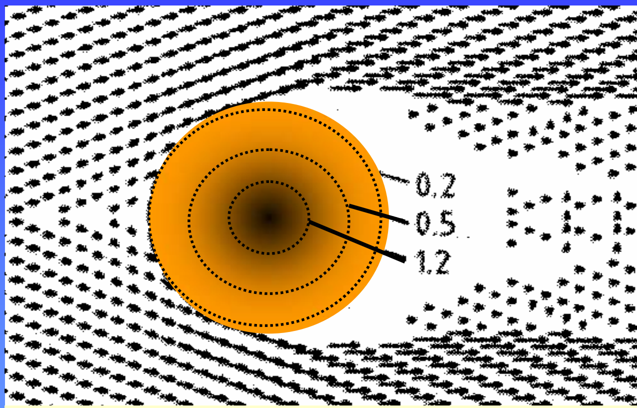

The subsonic plasma flow (M_s = 0.4) is accelerated and deflected by the heavy-ion cloud in regions where its density is about 0.2 n_{p0} .

Two-fluid modeling of SW-heavy ion source interaction: B=0

M_s=4

solar wind

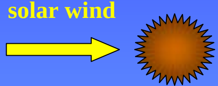

heavy-ion source:
$q=q_m \cdot \exp(-r^2/L^2)$

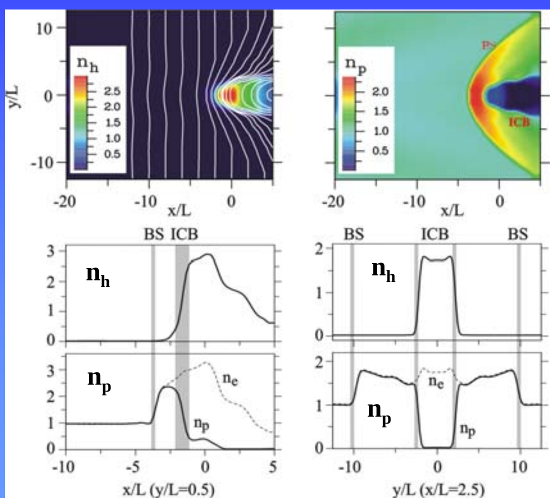

Formation of a proton cavity

Observation of sharp boundaries in dusty plasmas under micro-gravity

(Annaratone et al., 2002)

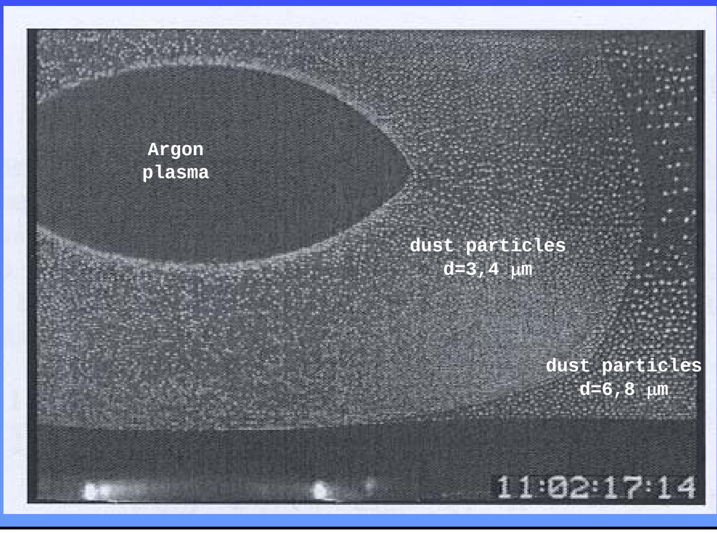

Observation of sharp boundaries in dusty plasmas under micro-gravity

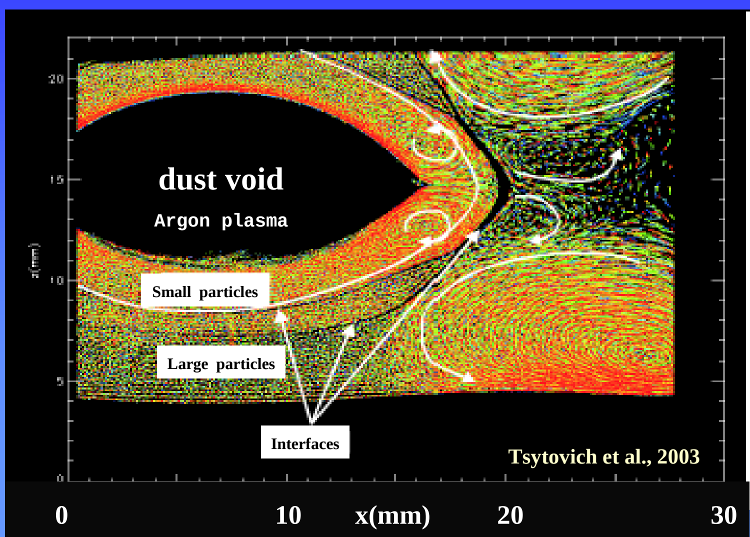

MISPR

Summary and conclusion

•The multi-fluid model is able to describe essential elements of solar wind interaction with non-magnetized bodies.

•The transition from very asymmetric plasma structures at weak comets to the magnetosphere of Mars with three well developed plasma boundaries (BS, ICB/MPB, IP) has been shown.

•The Ion Composition Boundary (ICB/MPB) at comets and Mars is a new type of plasma boundary which is formed in mass-loaded plasmas. It results from the momentum coupling between the two plasma populations at the "generalized sonic points".

MISPR

Summary and conclusion

The results have implications to future space missions:

•ROSETTA
In-situ measurements near a (weak) comet at ~ 3AU.

•MARS/VENUS EXPRESS
Plasma and neutral gas measurements with ASPERA-3.

•CASSINI
New results about solar wind -Titan interaction.

•Beppi Colombo
Mercury with its sodium atmosphere is an interesting multi-ion object.

Summary and conclusion

- The work was done in the project "Mars, Kometen, kleine Körper"
- ~25 publications in 2000-2003
- low costs: ≤ 2 000 EU per annum (contacts to ISSI, CNRS, JPL)